RANGE CONTROL DURING INITIAL PHASES OF SUPERCIRCULAR REENTRIES

by

Donald Louis Baradell

Thesis submitted to the Graduate Faculty of the

Virginia Polytechnic Institute

in candidacy for the degree of

MASTER OF SCIENCE

in

AEROSPACE ENGINEERING

May 1962

Blacksburg, Virginia

II. TABLE OF CONTENTS

III. LIST OF FIGURES

IV. INTRODUCTION

The successful completion of any manned space mission implies the solution of two general problems - survival of the extreme heating and deceleration loads of reentry, and vehicle recovery. The survival problem implies the return of the vehicle to the earth's surface within vehicle and passenger tolerance limits. Most reentry research to date (some of which is covered in refs. 1-20) has focused on this problem. The recovery problem implies the ability to return the vehicle to some desired point on the earth's surface. For direct reentry from a near lunar or a deep space mission, considerable variations in reentry point, reentry angle and reentry plane must be anticipated. The reentry vehicle must, therefore, possess the ability to control its range after reentry in order to achieve the desired point return. Aerodynamic maneuvering can provide the desired control of range.

Recent studies have indicated that considerable ranges can be achieved by even low L/D vehicles ($0 < L/D \leq 1$), operating wholly within the atmosphere, if proper maneuvering is accomplished early in the reentry, while the vehicle is still traveling at supercircular speeds. Several modes of operation which are capable of providing range control at supercircular speeds are discussed in references 21 and 22. In reference 21, idealized maneuvers for achieving maximum and minimum ranges from given initial conditions are discussed, and approximate equations for these ranges are presented. In addition, reference 21 presents preliminary results obtained in a six-degree-of-freedom fixed base analog simulator at the Langley Research Center. These results indicate that a human pilot can perform satisfactorily the basic maneuvers required for range control at supercircular speeds.

These recent studies have considered initiating range control while the vehicle is traveling at supercircular speeds, but only after the initial pull-up has been performed; that is, after the initial flight-path angle has been reduced to zero. In considering longitudinal range, not much is lost in most cases by delaying range control until after the pull-up is completed, since the range during pull-up comprises a small portion of the total achievable range. In considering lateral range control, however, small changes in heading angle during the initial pull-up can result in large lateral displacements of the landing point.

The present investigation will explore the possibility of increasing the lateral range capability of reentry vehicles by allowing the vehicle to reenter the atmosphere in a banked attitude. The vehicle considered will utilize the "roll only" maneuver discussed in references 21 and 22. Equations will be developed for the motion of a vehicle entering the atmosphere of a spherical nonrotating earth and some permissible approximations to these equations will be discussed. The effects of the banked reentry on the allowable supercircular reentry corridor and on the vehicle lateral range capability will be determined. Numerical results obtained for the developed system of equations through use of an IBM 7090 high-speed computer will be used throughout the investigation to furnish accurate evaluations of the effects in question and to check the validity of the approximations used.

V. SYMBOLS

A	reference area
a_{ij}	metric tensor
C_D	drag coefficient (eq. 20)
c.w.	corridor width
D	drag force
F_k	tensor components of external force
$F_{(k)}$	physical components of external force
g	acceleration due to gravity
h	altitude above earth's surface
L	lift force
L_V	vertical component of lift force (eq. 1)
L_Y	lateral component of lift force (eq. 1)
m	mass of vehicle
R	resultant force
r	distance from center of earth
r_{atm}	distance from center of earth to edge of appreciable atmosphere
r_p	distance from center of earth to perigee of orbit
T	kinetic energy (eq. 3)
t	time
V	total velocity
V_k	tensor components of velocity
$V_{(k)}$	physical components of velocity
W	vehicle weight (= mg)
x^k	general coordinates (k = 1, 2, 3)

γ	flight-path angle (eq. 12)
$\Delta\lambda$	lateral range increment
$\Delta\xi$	heading angle change
ϵ	eccentricity of orbit
θ	angular polar coordinate
λ	lateral displacement angle (fig. 1)
ξ	heading angle (eq. 12)
ρ	density of atmosphere
φ	bank angle
ψ	longitudinal range angle (fig. 1)
ψ_c	range available after completion of initial pull-up

Subscripts:

o	initial reentry conditions
e	evaluated at earth's surface
i, j, k	suffixes in range and summation convention (= 1, 2, 3)
ov	overshoot conditions
un	undershoot conditions
$(\dot{\ })$	indicates differentiation with respect to time

VI. THEORETICAL MODEL CONSIDERED

This investigation will consider the motion of a vehicle reentering the atmosphere of a spherical nonrotating earth under the influence of aerodynamic and gravitational forces. The simplified earth model was considered in this parametric study in order that results of a more general nature might be obtained. If the additional forces due to the rotation and oblateness of the earth are considered, separate solutions would be required for each reentry point and reentry direction. Any trajectory calculations of a final, specific nature should, of course, include these forces. For the simplified model used in this investigation, the reentry solutions are independent of the specific point and direction of reentry, and no generality is lost by assuming the reentry to occur in the equatorial plane.

The vehicle considered will be an approximately flat-face type, which utilizes the roll only mode of maneuvering discussed in references 21 and 22. A constant angle of attack, corresponding to vehicle maximum L/D, is maintained throughout the portion of the reentry considered. The resultant aerodynamic force is composed of a drag force opposite to the direction of motion, and a lift force normal to the drag. By banking the vehicle, the lift force (L) is rotated about the drag force (D) giving rise to vertical and horizontal components of lift, defined in terms of the bank angle φ.

$$\left.\begin{aligned} L_V &= L \cos \varphi \\ L_Y &= L \sin \varphi \end{aligned}\right\} \qquad (1)$$

By proper variation of the bank angle, any desired values of L_V/D or L_Y/D from $-(L/D)$ to $+(L/D)$ can be obtained.

This mode of operation is attractive from both the point of view of simplifying heat protection requirements and from the standpoint of attitude control, as discussed in reference 21. The appropriate pitch for the desired L/D would be selected prior to reentry and the vehicle would be trimmed in this attitude by either an offset center of gravity or a fixed aerodynamic flap type of pitch control (or a combination of the two). Variation of the vertical component of lift as necessary throughout the reentry can be accomplished by rolling the vehicle about the wind axis. The lateral displacement introduced by such a maneuver can be corrected for, if it is so desired, by alternating the direction of roll so as to affect a weaving motion about the desired flight path. For the type of vehicle considered, rolling moments are low and roll control could be accomplished economically by use of the same reaction jet system used for roll stabilization in space. This is generally not possible for pitch control due to the relatively large pitching moments involved. Artificial damping would be included about all three axes.

VII. REENTRY EQUATIONS

A. Coordinate System

The spherical coordinate system chosen for use in this investigation is indicated in figure 1. The position of the vehicle at any time is determined by the coordinates r, λ, and ψ. If the $\lambda = 0$ plane is taken as the equatorial plane, then λ corresponds to the geographical latitude and ψ is a measure of the geographic longitude on the earth's surface. Throughout this investigation, the reentry point is assumed given by $\lambda_o = \psi_o = 0$ and $r_o = (r_e + h_{atm})$ where r_e is the radius of the earth and h_{atm} is the height of the appreciable atmosphere, taken as 400,000 ft.

B. Derivation of Equations of Motion

The Lagrangian equations for the motion of a particle under the influence of external forces can be written in index notation as (ref. 23)

$$\frac{d}{dt}\left(\frac{\partial T}{\partial \dot{x}^k}\right) - \frac{\partial T}{\partial x^k} = F_k \tag{2}$$

The quantity T is the kinetic energy of the particle. The suffix k takes on the values 1, 2, 3 for the three-dimensional space considered. In general coordinates the kinetic energy is given by

$$T = \frac{m}{2} a_{ij}\dot{x}^i\dot{x}^j \tag{3}$$

where suffixes repeated an even number of times indicate summation and the dot indicates differentiation with respect to time. The derivatives of T are therefore

$$\frac{\partial T}{\partial \dot{x}^k} = m a_{ik} \dot{x}^i \tag{4}$$

$$\frac{\partial T}{\partial x^k} = \frac{m}{2} \dot{x}^i \dot{x}^j \frac{\partial a_{ij}}{\partial x^k} \tag{5}$$

and the equations of motion can be written

$$m \frac{d}{dt}(a_{ik} \dot{x}^i) - \frac{m}{2} \dot{x}^i \dot{x}^j \frac{\partial a_{ij}}{\partial x^k} = F_k \tag{6}$$

For the coordinate system used here, the metric tensor is

$$a_{ij} = \begin{pmatrix} 1 & 0 & 0 \\ 0 & (x^1)^2 & 0 \\ 0 & 0 & (x^1 \cos x^2)^2 \end{pmatrix} \tag{7}$$

where $x^1 = r$, $x^2 = \lambda$, $x^3 = \psi$.

F_k are the covariant tensor components of the external forces acting on the vehicle and are related to the physical force components $(F_{(k)})$ by the expression

$$F_k = \sqrt{a_{kk}} F_{(k)} \tag{8}$$

The contravariant tensor components of the velocity are given by

$$V^k = \dot{x}^k \tag{9}$$

and are related to the physical velocity components $(V_{(k)})$ through the expression

$$V_{(k)} = \sqrt{a_{kk}}V^k = \sqrt{a_{kk}}\dot{x}^k \tag{10}$$

The total velocity is given by

$$V = \sqrt{V_{(k)}V_{(k)}} = \sqrt{(\dot{r})^2 + (r\dot{\lambda})^2 + (r \cos \lambda\dot{\psi})^2} \tag{11}$$

If we introduce the flight-path angle (γ) and the heading angle (ξ) defined by (see fig. 1)

$$\begin{aligned} \gamma &= \sin^{-1} \frac{V_{(r)}}{V} = \sin^{-1} \frac{\dot{r}}{V} \\ \xi &= \tan^{-1} \frac{V_{(\lambda)}}{V_{(\psi)}} = \tan^{-1}\left(\frac{r\dot{\lambda}}{r \cos \lambda\dot{\psi}}\right) \end{aligned} \tag{12}$$

from equations (11) and (12) we can write

$$\left.\begin{aligned} \dot{r} &= V \sin \gamma \\ \dot{\psi} &= \frac{V \cos \gamma \cos \xi}{r \cos \lambda} \\ \dot{\lambda} &= \frac{V \cos \gamma \sin \xi}{r} \end{aligned}\right\} \tag{13}$$

Differentiating equations (13) yields

$$\begin{aligned} \ddot{r} &= \dot{V} \sin \gamma + \dot{\gamma}V \cos \gamma \\ \ddot{\psi} &= \frac{1}{r \cos \lambda}\left[\dot{V} \cos \gamma \cos \xi - \dot{\xi}V \cos \gamma \sin \xi - \dot{\gamma}V \sin \gamma \cos \xi \right. \\ &\quad \left. + \frac{(V \cos \gamma)^2}{r}(\sin \xi \cos \xi \tan \lambda - \tan \gamma \cos \xi)\right] \\ \ddot{\lambda} &= \frac{1}{r}\left[\dot{V} \cos \gamma \sin \xi + \dot{\xi}V \cos \gamma \cos \xi - \dot{\gamma}V \sin \gamma \sin \xi - \frac{V^2}{r} \sin \gamma \cos \gamma \sin \xi\right] \end{aligned} \tag{14}$$

The physical components of the external forces are given by

$$\left.\begin{aligned} F_{(r)} &= L \cos \varphi \cos \gamma - D \sin \gamma - mg \\ F_{(\lambda)} &= -L \cos \varphi \sin \gamma \sin \xi + L \sin \varphi \cos \xi - D \cos \gamma \sin \xi \\ F_{(\psi)} &= -L \cos \varphi \sin \gamma \cos \xi - L \sin \varphi \sin \xi - D \cos \gamma \cos \xi \end{aligned}\right\} \qquad (15)$$

where L and D are the aerodynamic lift and drag forces, respectively, and φ is the vehicle bank angle. (See fig. 1.)

Substituting equations (7) and (8) into equation (6) we obtain

$$\left.\begin{aligned} \ddot{r} - r(\dot{\lambda})^2 - r \cos^2\lambda(\dot{\psi})^2 &= \frac{F(r)}{m} \\ r\ddot{\lambda} + 2\dot{\lambda}\dot{r} + r \sin \lambda \cos \lambda(\dot{\psi})^2 &= \frac{F(\lambda)}{m} \\ r \cos \lambda\ddot{\psi} + 2 \cos \lambda\dot{\psi}\dot{r} - 2r \sin \lambda\dot{\psi}\dot{\lambda} &= \frac{F(\psi)}{m} \end{aligned}\right\} \qquad (16)$$

If equations (13), (14), and (15) are then substituted into equation (16) three equations in $\dot{V}$, $\dot{\gamma}$, and $\dot{\xi}$ are obtained which can be solved to yield

$$\begin{aligned} \dot{V} &= -\frac{D}{m} - g \sin \gamma \\ \dot{\gamma} &= \frac{L \cos \varphi}{mV} - \frac{g \cos \gamma}{V} + \frac{V \cos \gamma}{r} \\ \dot{\xi} &= \frac{L \sin \varphi}{mV \cos \gamma} - \frac{V \cos \gamma \tan \lambda \cos \xi}{r} \end{aligned} \qquad (17)$$

Equations (13) and (17) provide us with six equations in six dependent variables $(r, \psi, \lambda, V, \gamma, \xi)$. The quantities $\frac{L}{D}$, $\frac{W}{C_D A}$, and

and φ are considered given. The variables ρ and g can be related to r through the relations

$$g = g_e\left(\frac{r_e}{r}\right)^2 \tag{18}$$

$$\rho = \rho(h) = \rho(r - r_e) \tag{19}$$

where r_e is the radius of the earth and g_e is the acceleration of gravity at the earth's surface. An appropriate density-altitude relation is chosen for equation (19).

Introducing the drag coefficient defined by

$$C_D \equiv \frac{D}{\frac{1}{2}\rho V^2 A} \tag{20}$$

and the vehicle weight $W(= mg)$ the complete system of equations can be written as

$$\frac{1}{g}\frac{dV}{dt} = -\frac{1}{2}\rho V^2\left(\frac{C_D A}{W}\right) - \sin\gamma \tag{21}$$

$$\frac{1}{g}\frac{d\gamma}{dt} = \frac{1}{2}\rho V\left(\frac{C_D A}{W}\right)\frac{L}{D}\cos\varphi - \frac{\cos\gamma}{V}\left[1 - \frac{V^2}{gr}\right] \tag{22}$$

$$\frac{1}{g}\frac{d\xi}{dt} = \frac{1}{2}\rho V\left(\frac{C_D A}{W}\right)\frac{L}{D}\frac{\sin\varphi}{\cos\gamma} - \frac{V}{gr}\cos\gamma\cos\xi\tan\lambda \tag{23}$$

$$\frac{d\psi}{dt} = \frac{V\cos\gamma\cos\xi}{r\cos\lambda} \tag{24}$$

$$\frac{d\lambda}{dt} = \frac{V \cos \gamma \sin \xi}{r} \tag{25}$$

$$\frac{dr}{dt} = V \sin \gamma \tag{26}$$

$$\rho = \rho(h) = \rho(r - r_e) \tag{27}$$

$$g = g_e\left(\frac{r_e}{r}\right)^2 \tag{28}$$

C. Method of Numerical Solution

These equations are readily amendable to numerical solution by a finite difference procedure. For the numerical results presented in this thesis, these equations were programed for the IBM 7090 high-speed computer in the Analytical Computing Section of the Langley Research Center. The solution was obtained by considering an incremental increase of time, the length of which was allowed to vary in order to assure sufficient linearity of all dependent variables over the time increment considered. For these numerical calculations the 1959 ARDC model atmosphere (ref. 24) was used. All numerical results presented in this thesis are for a vehicle reentering the atmosphere at escape velocity ($V_o = 36{,}500$ fps) and for a vehicle W/C_DA of 50 psf, which value is appropriate for manned vehicles in the L/D range considered.

VIII. REENTRY CORRIDOR

The velocity of a vehicle reentering from a circular near-earth orbit is less than circular orbital velocity at all times during the reentry. The force of gravity, therefore, exceeds the centrifugal force acting on the vehicle, and the vehicle tends to return to the earth's surface. The survival problem for such a reentry is to avoid excessive deceleration loads or aerodynamic heating - that is, to avoid entering too steeply.

In reentering from a lunar or deep space mission, the vehicle possesses greater than circular satellite velocity. The centrifugal force is greater than the force of gravity, and the vehicle tends to skip back out of the atmosphere. For such reentries, a second limitation is placed on the reentry angle - if the path is too shallow the vehicle will not penetrate the atmosphere deeply enough to lose much velocity, and will skip back out into space. These two limitations define a narrow range of permissible reentry angles which determine the allowable reentry corridor for supercircular reentries. The corridor width is effectively the distance between the return orbits which will intersect the atmosphere at the maximum and minimum angles which will permit successful reentry.

The relation between the permissible spread of reentry angles and the corridor width can be obtained from simple geometric considerations. The equations of the orbit for a two-body central force problem, where the force of attraction is inversely proportional to the square of the distance from the origin of the attracting force, is the equation of a conic with the origin at one focal point. In polar coordinates (r, θ), this can be written

$$\frac{r}{r_p} = \frac{1 + \epsilon}{1 + \epsilon \cos \theta} \tag{29}$$

where r_p is the distance to perigee, θ is measured from the perigee position, and ϵ is the eccentricity of the orbit.

The outer limit of the atmosphere is given by $r = r_{atm}$ = constant.

The angle of intersection of two curves in polar coordinates is given by

$$\tan \gamma = \frac{r_1 r_2' - r_2 r_1'}{r_1' r_2' + r_1 r_2} \tag{30}$$

where the prime indicates differentiation with respect to θ. If $r_2 = r_{atm}$ then $r_2' = 0$ and equation (30) becomes

$$\tan \gamma_o = -\frac{r_1'}{r_1} = \frac{\epsilon \sin \theta_o}{1 + \epsilon \cos \theta_o} \tag{31}$$

For the case of a parabolic (escape) orbit, $\epsilon = 1$, and from equation (31)

$$\gamma_o = \frac{\theta_o}{2} \tag{32}$$

The perigee distance can then be written in terms of reentry angle as

$$r_p = r_{atm}\left(\frac{1 + \cos 2\gamma_o}{2}\right) \tag{33}$$

The corridor width (c.w.) is defined as the difference between the perigee distances for overshoot and undershoot. For a parabolic reentry this is

$$r_{p_{ov}} - r_{p_{un}} = \frac{r_{atm}}{2}(\cos 2\gamma_{ov} - \cos 2\gamma_{un}) \tag{34}$$

which can be written

$$c.w. = r_{atm}(\sin^2\gamma_{un} - \sin^2\gamma_{ov}) \tag{35}$$

The reentry corridor, as used in this thesis, is defined by the following limits: The undershoot limit is taken as the steepest angle at which the vehicle can enter at a constant positive value of L_V/D without exceeding an acceleration of 10g. The overshoot limit is taken as the shallowest angle at which the vehicle can enter at a constant negative value of L_V/D so that at the bottom of pull-up, ($\gamma = 0$), the vehicle can hold a constant altitude by rolling to full negative $L_V/D(\varphi = 180^\circ)$. The constant altitude requirement for the overshoot limit is based on the results of simulator studies, reference 21, which indicate that for shallow reentry angles, control becomes difficult if even a small positive flight-path angle is allowed to develop after pull-up.

The available reentry angle spread for unbanked low L/D vehicles reentering the atmosphere at escape speed is shown in figure 2. For these reentries, the undershoot limit corresponds to reentry at $L_V/D = L/D$, and the overshoot limit to reentry at $L_V/D = -L/D$. The corridor width resulting from these limiting angles as computed from equation (35) is shown on figure 3.

As can be seen from figures 2 and 3, the corridor width is a strong function of L/D, especially for the low values considered. At $L/D = 0.5$ the reentry corridor width is 4.5 times the nonlifting corridor width, while at $L/D = 1$, the width is about 5.5 times the nonlifting width. Most of the effect of L/D, in increasing corridor width, is thus achieved by values of L/D less than unity. The present investigation will be limited to values of L/D in this range, with particular concentration on vehicles with $L/D = 0.5$.

IX. EFFECTS OF BANKED REENTRY ON REENTRY CORRIDOR

A. Effect on Undershoot Limit

Since corridor width is strongly dependent on vehicle L_V/D, it is directly affected by the use of bank during reentry. A vehicle of given L/D, entering in a banked attitude, will follow the descent path of a lower L/D unbanked vehicle with the same value of L_V/D. The resultant force R acting on a vehicle is, however, dependent on the vehicle total L/D. This force is given by

$$\frac{R}{W} = \frac{1}{2} \rho V^2 \frac{C_D A}{W} \sqrt{1 + \left(\frac{L}{D}\right)^2} \tag{36}$$

The dynamic pressure $\frac{1}{2} \rho V^2$ is dependent only on the descent path for vehicles of equal $\left(\frac{W}{C_D A}\right)$. The banked vehicle considered above will, therefore, experience greater resultant loads, due to its higher L/D, than the lower L/D unbanked vehicle of equal L_V/D. Conversely, the reentry angle for a 10g deceleration limit will be shallower for the banked vehicle. The extent to which banking affects the undershoot limit for a parabolic reentry is indicated in figure 4. The reentry angle which will produce a maximum deceleration of 10g is plotted against the L_V/D employed.

Reentries over a range of entry angles were considered for vehicles with L/D between zero and one and values of φ from 0° to 90°. The solid line shows the limiting undershoot angles for unbanked vehicles. The dashed lines show the limits for vehicles with $L/D = 0.5$ and 1, which reenter at various bank angles φ to vary the value of L_V/D.

As can be seen, the limiting angles for a $L/D = 0.5$ banked vehicle are only slightly less than those for an unbanked vehicle entering at the same L_V/D. For the $L/D = 1$ banked reentry, the differences are considerably larger.

B. Effect on Overshoot Limit

If operation near the overshoot limit is considered, negative lift is required in order to overcome the tendency of the vehicle to skip out of the atmosphere. At any given altitude and velocity, a vehicle operating at full negative $L_V/D(\varphi = 180^o)$ obviously employs more force in the earthward direction than a vehicle of the same L/D operating at a lesser bank angle.

On the other hand, consider the reentry of two vehicles operating at different values of L/D but at the same negative value of L_V/D. This could be the case if the higher L/D vehicle reenters at some bank angle between 90^o and 180^o, and the lower L/D vehicle reenters at $\varphi = 180^o$. The descent paths of the two vehicles during the initial pull-up would be identical. At the bottom of the pull-up, however, the higher L/D vehicle would have the capability of rolling to $\varphi = 180^o$ in order to exert more force earthward than the lower L/D vehicle which is already at full negative L_V/D. Thus the higher L/D vehicle could maintain constant altitude after pull-up for shallower reentries than the lower L/D vehicle performing the same pull-up. In other words, a higher L/D banked vehicle can successfully reenter at shallower angles than a lower L/D unbanked vehicle reentering at the same value of L_V/D. This is illustrated in figure 5, which shows the variation of corridor overshoot limit with vehicle L_V/D. The solid line applies to a vehicle employing full negative $L_V/D(\varphi = 180^\circ)$, and the dashed lines apply to vehicles with $L/D = 0.5$ and 1 which reenter at values of φ between 90° and 180°, thus achieving different values of L_V/D.

The comparison of banked and unbanked vehicles on the basis of the same L_V/D is not to be interpreted as a valid measure of the effect of bank on corridor width. Obviously, the true measure of this effect for a vehicle of given L/D capability is a comparison of corridor width for a vehicle utilizing bank with the corridor width for the same vehicle utilizing either full positive or full negative lift only. The purpose of presenting the results in the form of a comparison on the basis of L_V/D is to show how the reduction in corridor width due to bank compares with the reduction that would be expected due to the lower effective lift force.

From figures 4 and 5 we can obtain the allowable span of reentry angles for banked and unbanked $(\cos \varphi = \pm 1)$ vehicles as presented in figure 6. While the $L/D = 1$ vehicle shows a considerably smaller span for the banked case, the variation for the $L/D = 0.5$ banked vehicle is seen to follow the unbanked variation quite closely. At the same time, the banked vehicle is also generating a lateral force which can be useful in extending lateral range capability.

X. EFFECT OF BANKED PULL-UP ON LATERAL RANGE

A. Lateral Force and Heading Angle Change During Pull-Up

In considering the development of lateral range and change in heading angle during the initial pull-up, it is to be noted from the foregoing discussion that the amount of lift available for lateral force depends on the position of the vehicle path in the reentry corridor. Near the extremes of this corridor, it is necessary to direct a certain amount of lift in the vertical direction to either alleviate the deceleration load or to avoid skipping. Some limitations are, therefore, placed on the bank angle that can be used near these extremes. The extent of these limitations for a vehicle with $L/D = 0.5$ reentering at escape speed is shown in figure 7. Near the overshoot limit, bank angles below the skip boundary, extending from $\gamma_o = -4.71$ to $\gamma_o = -5.02$, would allow insufficient lift in the earthward direction to prevent skipping. Near the undershoot limit, bank angles above the indicated deceleration boundary, extending from $\gamma_o = -5.87$ to $\gamma_o = -7.5$, would allow insufficient lift in the positive vertical direction and excessive deceleration would result. In the entry angle range from $\gamma_o = -5.02$ to $\gamma_o = -5.87$ the pull-up could be accomplished at maximum bank $(\varphi = 90^{\circ})$ without surpassing either corridor limit.

The amount of lateral force which is available to the above vehicle for the range of allowable reentry angles is presented in figure 8. Near maximum values of L_Y/D are seen to be available throughout much of the corridor.

The lateral force used produces a lateral displacement and a heading angle change. The lateral displacement which is obtained during the initial phases of reentry is small compared to the total lateral range which can be obtained. The heading angle change, however, can contribute significantly to the total lateral range as indicated in figure 9.

In this sketch, four reentry path traces are shown corresponding to different bank no-bank combinations. The quantity ψ_c is the longitudinal range available to the vehicle after pull-up, $\Delta\xi$ is the heading angle change obtained during pull-up, and $\Delta\lambda$ is the lateral range increment due to the use of bank during pull-up.

The trace OA corresponds to the path the vehicle would follow if no lateral displacement were desired. OC is the path for a vehicle banking after the initial pull-up only. OB corresponds to a vehicle banking during the initial pull-up but not after. OD is the trace of a vehicle using bank throughout the reentry. The trace OB indicates the manner in which bank during reentry can affect lateral range. Although the heading angle change during pull-up is small, considerable lateral range is obtained due to the characteristically large values of ψ_c. If the lateral displacement during pull-up is neglected, this lateral range increment is given by spherical trigonometry as

$$\tan(\Delta\lambda) = \tan(\Delta\xi)\sin\psi_c \tag{37}$$

B. Approximate Equation for Heading Angle Change

Throughout the initial phases of reentry, γ is small so that $\cos\gamma \approx 1$, $\sin\gamma \approx 0$. With these assumptions, equations (21), (23), and (24) become

$$\frac{dV}{dt} = -\frac{D}{m} \tag{38}$$

$$\frac{d\xi}{dt} = \frac{L \sin \varphi}{mV} - \frac{V}{r} \cos \xi \tan \lambda \tag{39}$$

$$\frac{d\psi}{dt} = \frac{V \cos \xi}{r \cos \lambda} \tag{40}$$

Combining equations (39) and (40) and using equation (1), there results

$$d\xi = \frac{L_Y}{mV} dt - \sin \lambda d\psi \tag{41}$$

The first term in this equation is the heading change due to aerodynamic forces, and the second term is due to the sphericity of the earth. For the moderate ranges and small lateral displacements achieved during the initial pull-up, this sphericity term may be neglected. If equation (41) is then combined with equation (38) there results

$$d\xi = -\frac{L_Y}{D} \frac{dV}{V} \tag{42}$$

which is readily integrated for constant L_Y/D to give

$$\xi = -\frac{L_Y}{D} \ln \frac{V}{V_o} \tag{43}$$

where integration is started at $V = V_o$ and $\xi = \xi_o = 0$. As a check on the validity of the approximations used, values obtained from equation (43) are compared with exact numerical values of ξ in figure 10. The numerical computations were for a vehicle with $L/D = 0.5$ reentering at escape velocity. The vehicle was banked prior to reentry and maintained a constant bank angle throughout the pull-up. The data points presented are conditions at the bottom of the pull-up for reentries throughout the allowable reentry corridor. The higher values of V for any given bank angle correspond to the shallower reentries.

For the $\varphi = 90^{\circ}$ cases, the last data point presented corresponds to the reentry in which satellite velocity is achieved at the bottom of pull-up. Beyond this value no pull-up point is defined as the flight-path angle will remain negative throughout the reentry. Good agreement between numerical results and values predicted by equation (43) is seen to exist for all cases considered.

The amount of heading angle change achieved during pull-up can also be obtained from figure 10. Values of ξ on the order of 0.05 radian are seen to be attainable throughout much of the corridor.

It should be noted that, in obtaining equation (43), the flight-path angle (γ) was taken to be approximately zero and effects of the earth's sphericity were neglected. Equation (43) is, therefore, the same equation as would be obtained for the heading angle change in planar, level flight. Although these approximations are valid for the initial phases of reentry, caution should be exercised in applying them to other portions of the trajectory where larger flight-path angles or ranges may be involved.

C. Evaluations of Lateral Range Increment

The lateral range increment due to banked reentry is directly dependent on the range the vehicle attains after pull-up (eq.(37)), and is thus dependent on the particular ranging maneuver employed. For a given ranging maneuver after pull-up, and a corresponding heading angle change prior to the start of that maneuver, the lateral range increment due to banked reentry can be evaluated. In figure 11, values of this increment, as given by equation (37), are presented for the range of the variables $\Delta\xi$ and ψ_c of interest.

In reference 21, lateral and longitudinal ranges are presented for vehicles performing two reentry maneuvers as a function of the velocity at which the maneuver is initiated. These maneuvers are begun shortly after pull-up. In figure 10 of this thesis, values of heading angle change developed by a vehicle in decelerating from reentry velocity to a given velocity are shown. Although the data points on figure 10 correspond to conditions at the bottom of pull-up, the curves presented are valid for some distance beyond this point, as long as the assumptions of small flight-path angle, small lateral displacement and moderate range apply.

These heading angle changes can be coupled with the ranges presented in figure 6 of reference 21 and this pair of values used in figure 11 of this thesis to evaluate the lateral range increment.

As an example, consider a vehicle of $L/D = 0.5$ reentering at a 60° bank angle and maintaining this attitude until $V = 31{,}000$ fps. From figure 10, the heading angle change developed to this point is about 0.052 radian. From figure 6 of reference 21 the range available from this point, using the maximum range mode of operation is about 1.5 earth radii. Entering figure 11 at $\psi_c = 1.5$, $\Delta\xi = 0.052$, one obtains a value of $\Delta\lambda$ of about 0.05 radian. This is the lateral range increment due to the banked pull-up considered. In figure 16 of reference 21, the lateral range available without a banked pull-up for this reentry is seen to be about 0.12 earth radii, so that the banked pull-up can provide about a 40-percent increase in lateral range for this case.

XI. CONCLUDING REMARKS

The feasibility of reentering from a supercircular orbit with a low L/D vehicle in a banked attitude has been studied. Emphasis was placed on reentry at escape velocity, but the effects determined for this case will also apply in character to reentry at other supercircular speeds.

The corridor limits for escape reentry were found to be affected by the banked pull-up in the manner expected. The limiting undershoot and overshoot angles for a banked vehicle were both found to be shallower than the corresponding limits for an unbanked vehicle with the same L_V/D and W/C_DA.

The variation of allowable reentry angle span with L_V/D for a banked vehicle with $L/D = 0.5$ was found to follow closely the variation with L_V/D appropriate to equivalent unbanked vehicles.

The amount of lateral force which can be used near the corridor extremes is limited by vertical lift requirements, but near maximum lateral force can be used throughout most of the corridor for a vehicle with $L/D = 0.5$.

The heading angle change developed during the initial pull-up by a vehicle reentering in a banked attitude can produce significant increases in the total lateral range achieved during the reentry.

XII. REFERENCES

1. Allen, H. Julian, and Eggers, A. J., Jr.: A Study of the Motion and Aerodynamic Heating of Ballistic Missiles Entering the Earth's Atmosphere at High Supersonic Speeds. NASA Rep. 1381, 1958.

2. Becker, John V.: Heating Penalty Associated With Modulated Entry Into Earth's Atmosphere. ARS Journal, May 1960, pp. 404-405.

3. Becker, John V.: Reentry From Space. Scientific American, vol. 204, no. 1, January 1961, pp. 51-57.

4. Bryson, A. E., Denham, W. F., Carroll, F. J., and Mikami, K.: Determination of the Lift or Drag Program That Minimizes Reentry Heating With Acceleration or Range Constraints Using a Steepest Descent Computation Procedure. Presented to the IAS 29th Annual Meeting, New York, Jan. 23-25, 1961.

5. Chapman, Dean R.: An Approximate Analytical Method for Studying Entry Into Planetary Atmospheres. NASA TR R-11, 1959.

6. Chapman, Dean R.: An Analysis of the Corridor and Guidance Requirements for Supercircular Entry Into Planetary Atmospheres. NASA TR R-55, 1959.

7. Detra, R. W., Riddell, F. R., and Rose, P. H.: Controlled Recovery of Non-Lifting Satellites. AVCO Rep. 54, May 1959.

8. Eggers, Alfred J., Jr., Allen, H. Julian, and Neice, Stanford E.: A comparative Analysis of the Performance of Long-Range Hypervelocity Vehicles. NACA Report 1382, 1958.

9. Grant, Frederick C.: Importance of the Variation of Drag With Lift in Minimization of Satellite Entry Acceleration. NASA TN D-120, 1959.

10. Grant, F. C.: Analysis of Low-Acceleration Lifting Entry From Escape Speed. NASA TN D-249, 1960.

11. Grant, F. C.: Modulated Entry. NASA TN D-452, 1960.

12. Hayes, J. E., Rose, P. H., and Vander Velde, W. E.: Analytical Study of a Drag Brake Control System for Hypersonic Vehicles. WADD Tech. Rep. 60-267, January 1960.

13. Lees, Lester: Reentry Heat Physics. Astronautics, March 1959. pp. 22-23.

14. Lees, Lester, Hartwig, Frederic W., and Cohen, Clarence B.: Use of Aerodynamic Lift During Entry Into the Earth's Atmosphere. ARS Journal, vol. 29, no. 9, 1959, pp. 633-641.

15. Luidens, Roger W.: Approximate Analysis of Atmospheric Entry Corridors and Angles. NASA TN D-590, 1961.

16. Robinson, Alfred C., and Besonis, Algimantas J.: On the Problems of Re-Entry Into the Earth's Atmosphere. WADC Tech. Rep. 58-408, Aug. 1958.

17. Schwaniger, Arthur J.: Use of Lift for Deceleration and Range Control for Reentry of Space Vehicles. Army Ballistic Missile Agency Rep. No. DA-TM-39-60, May 11, 1960.

18. Slye, Robert E.: An Analytical Method for Studying the Lateral Motion of Atmosphere Entry Vehicles. NASA TN D-325, 1960.

19. Ting, Lu: Some Aspects of Drag Reduction for Lifting Wing-Body Combinations at Supersonic Speed. PIBAL Report No. 445, May 1958.

20. Wong, Thomas J., and Slye, Robert E.: The Effect of Lift on Entry Corridor Depth and Guidance Requirements for the Return Lunar Flight. NASA TR R-80, 1960.

21. Becker, John V., Baradell, Donald L., and Pritchard, E. Brian: Aerodynamics of Trajectory Control for Reentry at Escape Speed. Astronautica Acta, vol. VII, Fasc. 5-6, 1961.

22. Mandell, Donald S.: Maneuvering Performance of Lifting Reentry Vehicles. ARS Journal, vol. 32, no. 3, March 1962.

23. Synge, J. L., and Schild, A.: Tensor Calculus. Toronto: University of Toronto Press, 1949.

24. Minzner, R. A., Champion, K. S. W., and Pond, H. L.: The ARDC Model Atmosphere, 1959. Air Force Surveys in Geophysics No. 115, Air Force Cambridge Research Center, Aug. 1959.

The vita has been removed from the scanned document

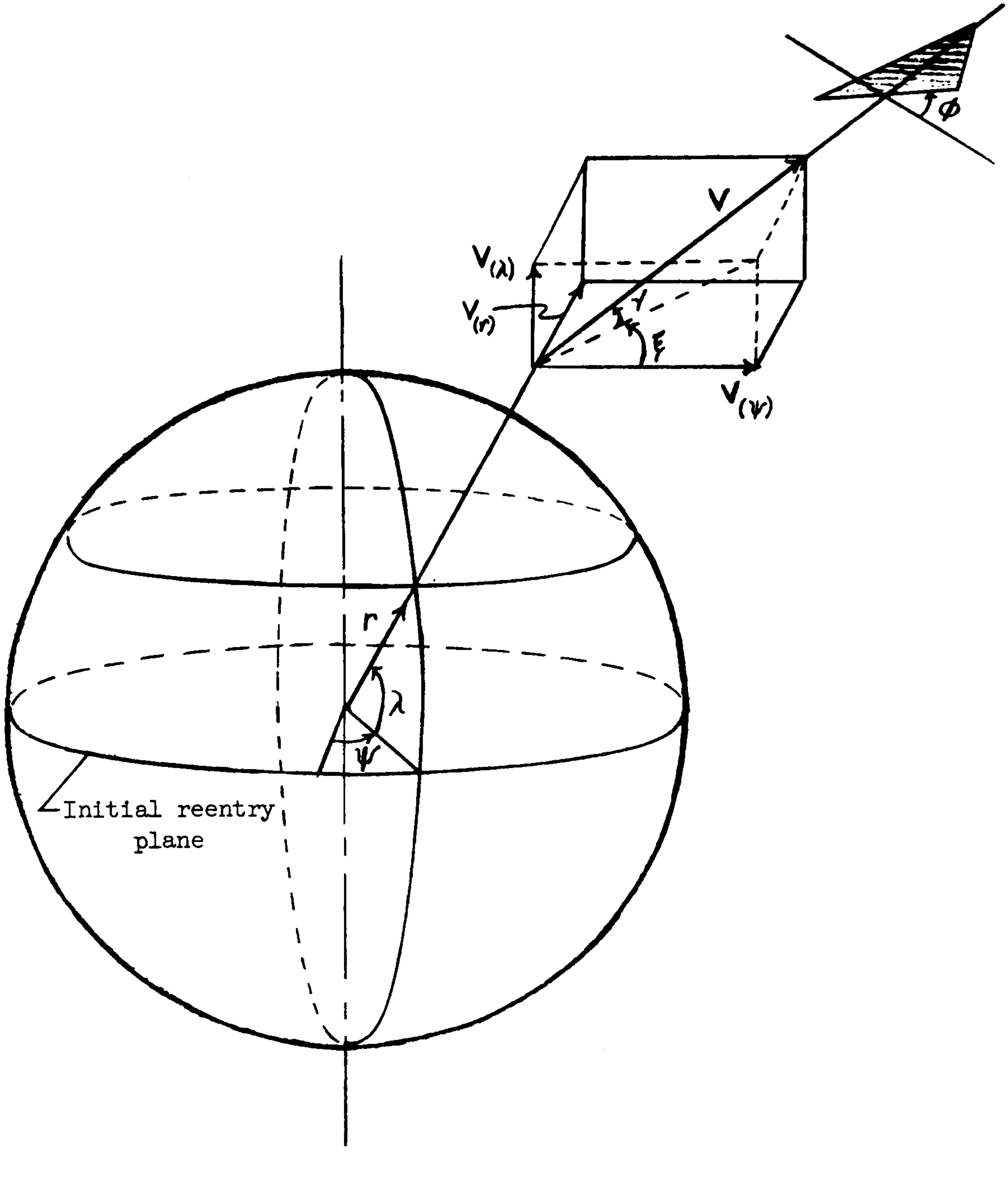

Figure 1.- Coordinate system for reentry equations.

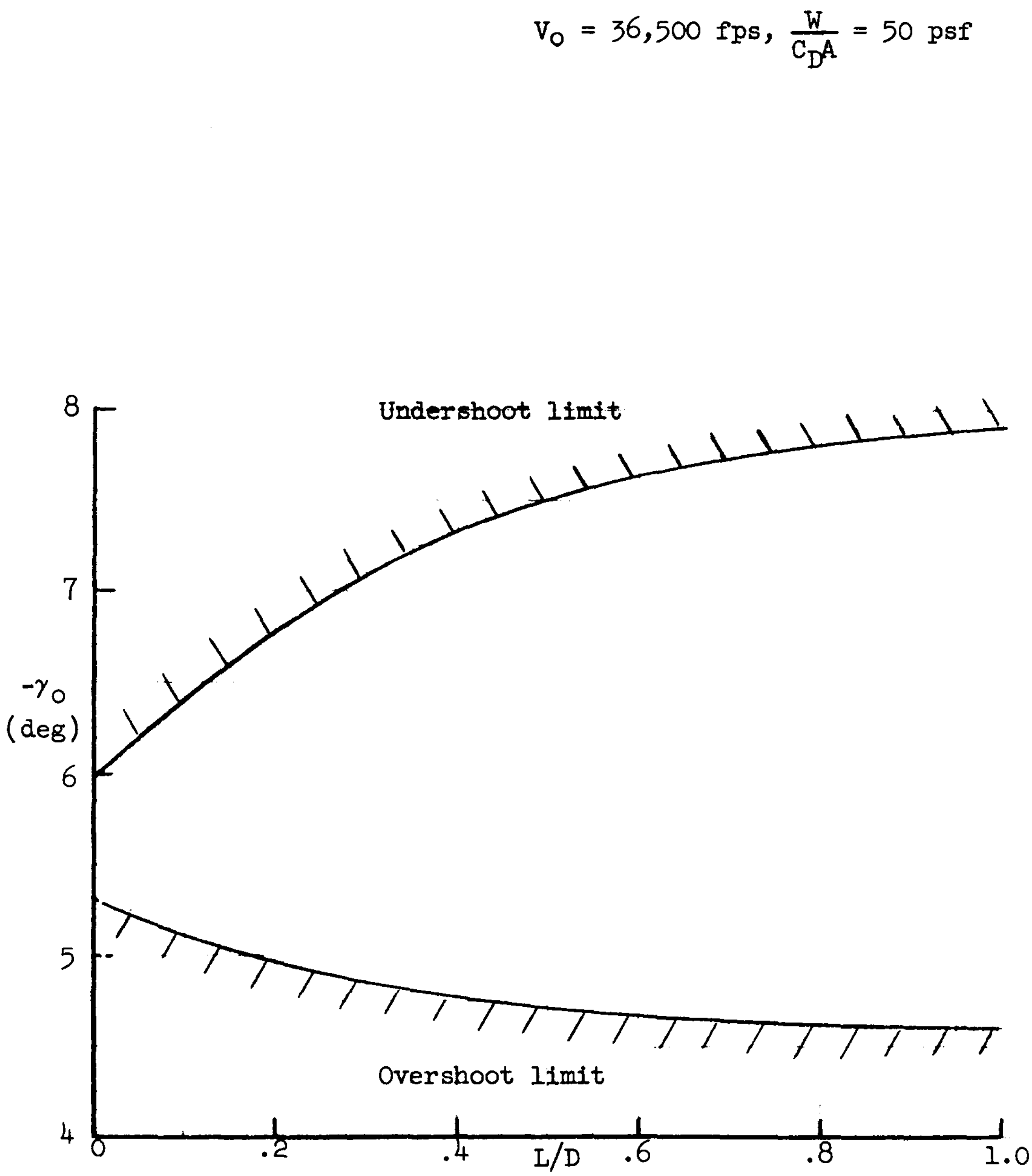

Figure 2.- Reentry angle limits.

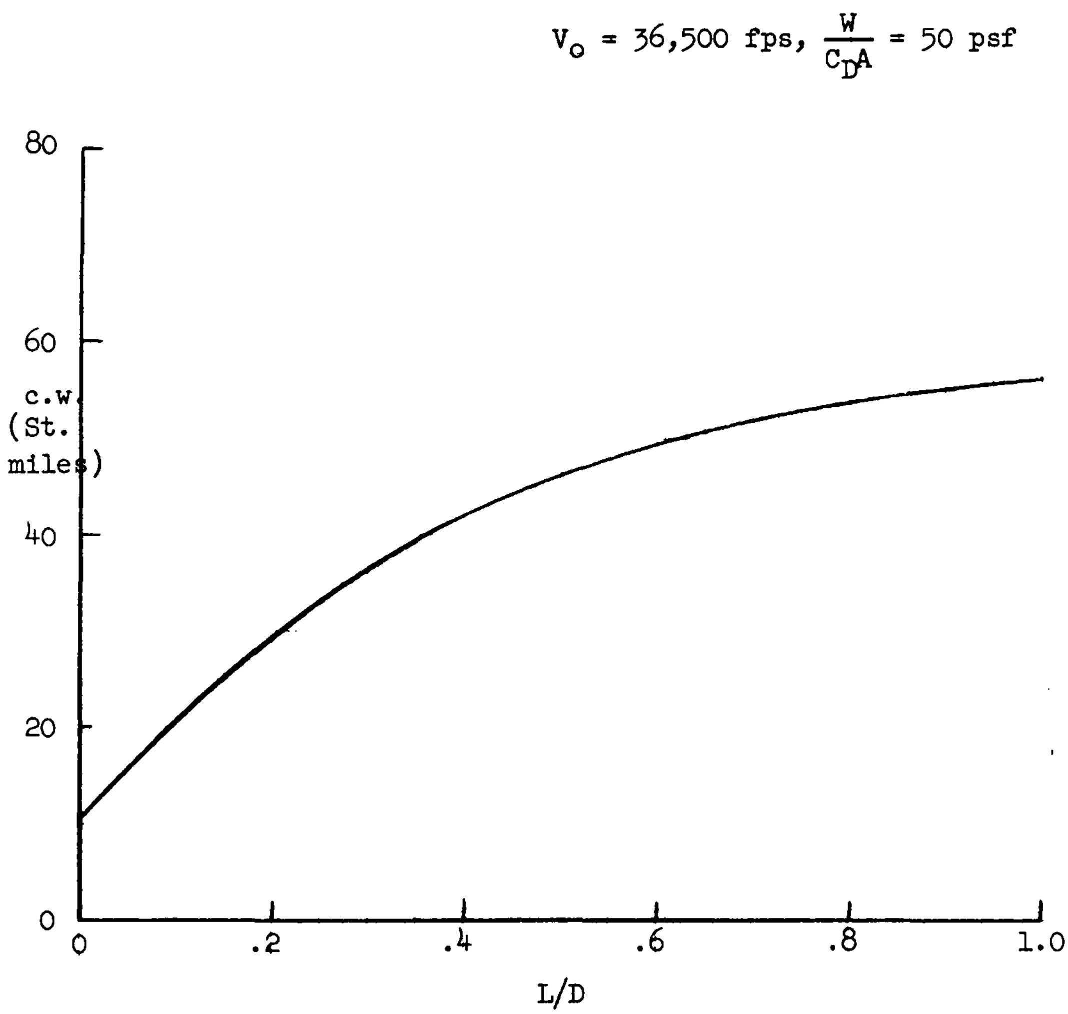

Figure 3.- Reentry corridor width.

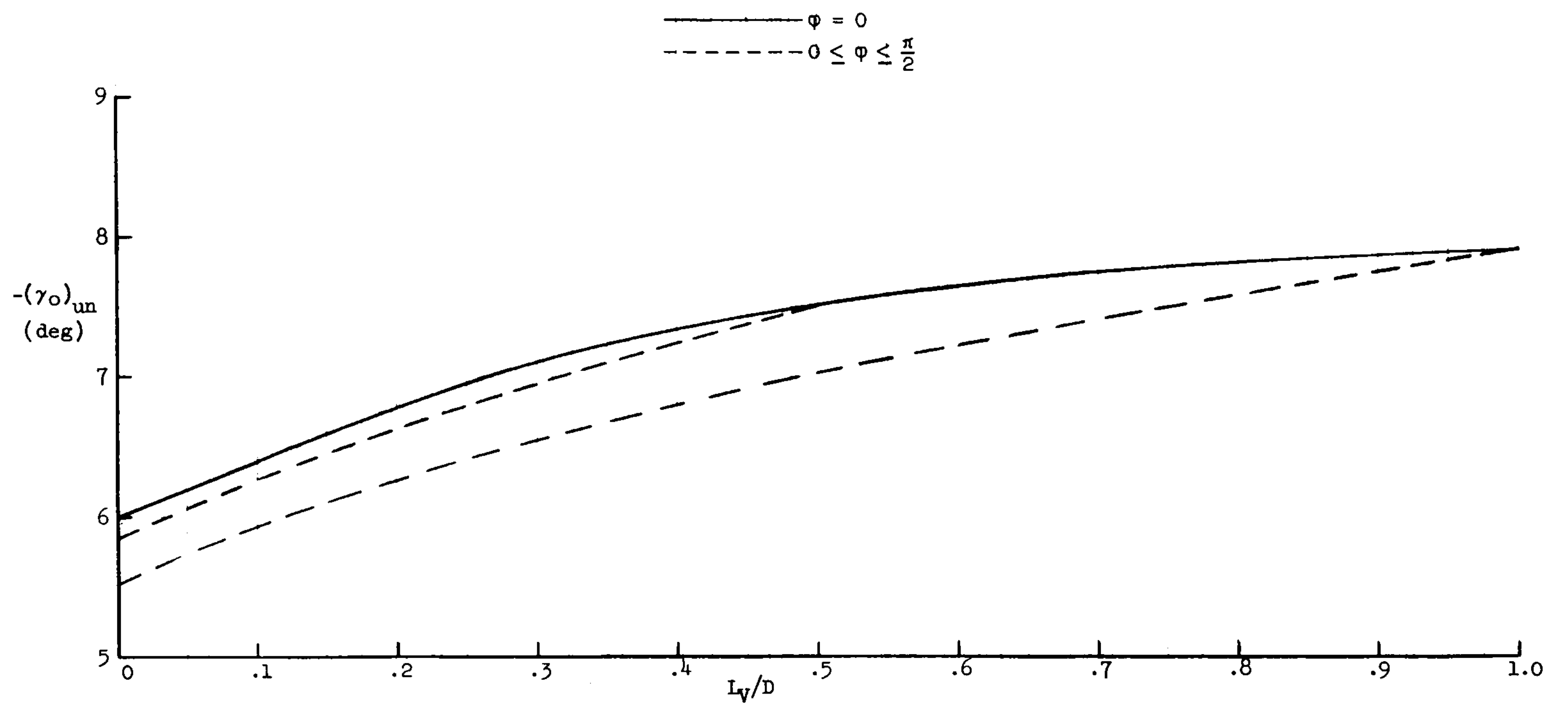

Figure 4.- Effect of banked reentry on undershoot limit.

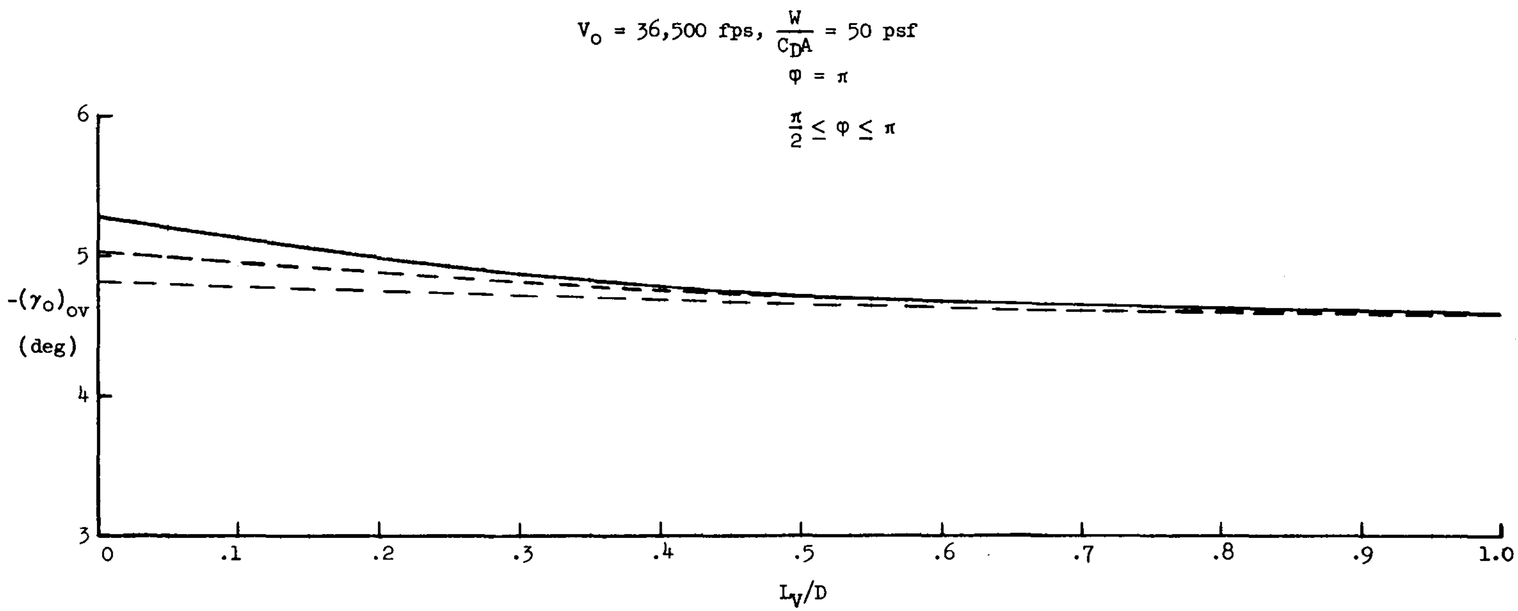

Figure 5.- Effect of banked reentry on overshoot limit.

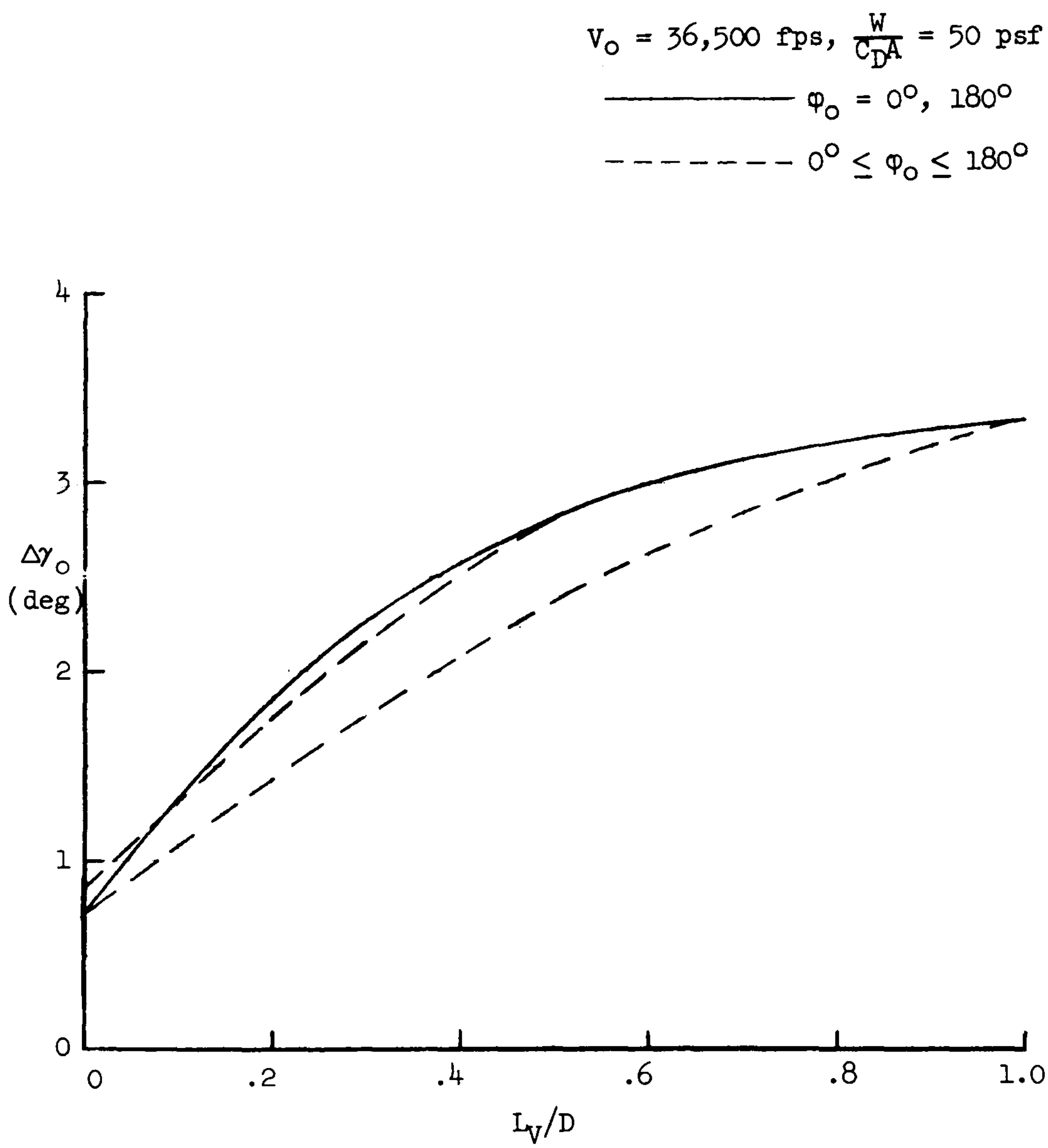

Figure 6.- Allowable span of reentry angle.

$\frac{L}{D} = 0.5$ $\quad V_i = 36{,}500$ fps

$\frac{W}{C_D A} = 50$ psf

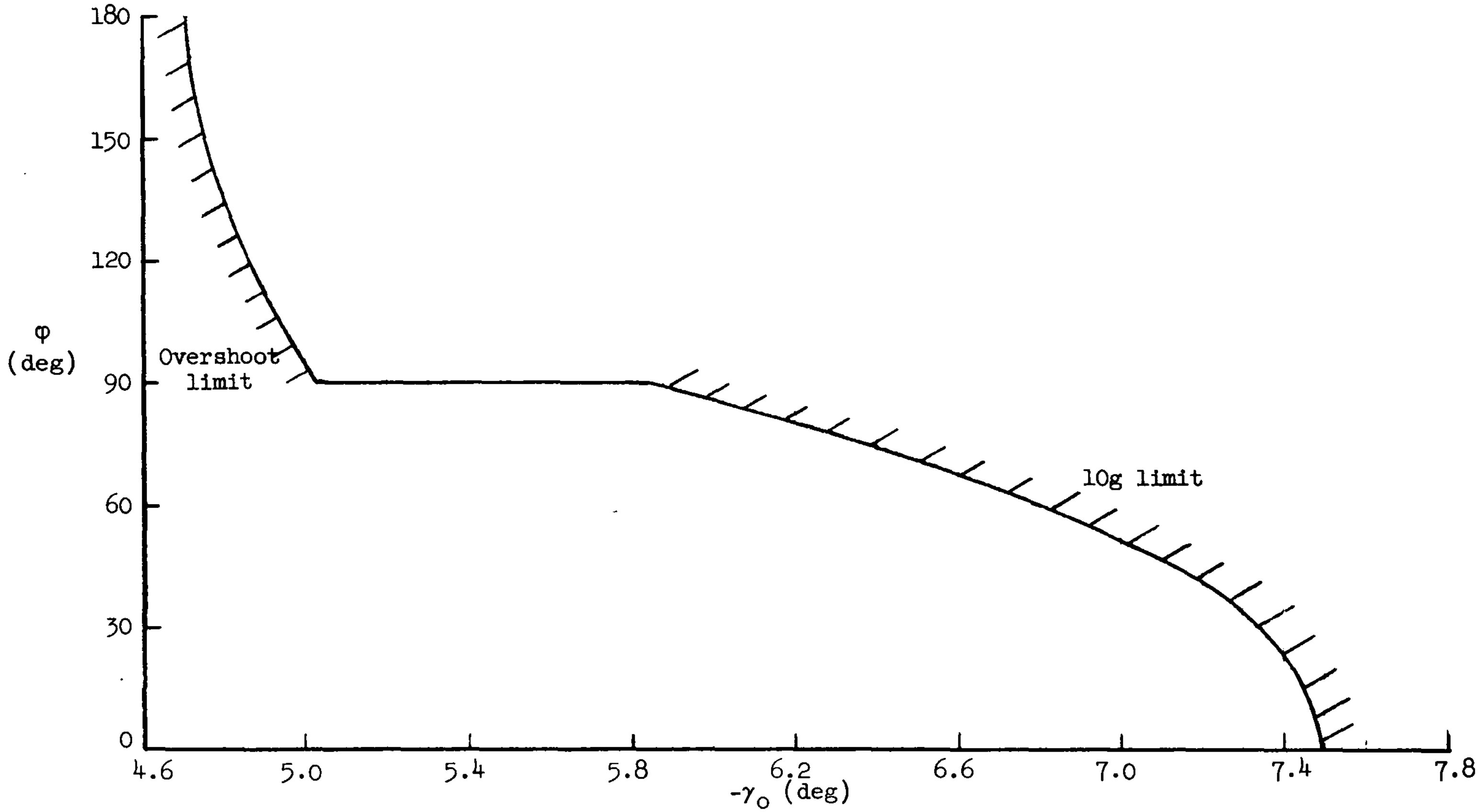

Figure 7.- Bank angle limits during pull-up.

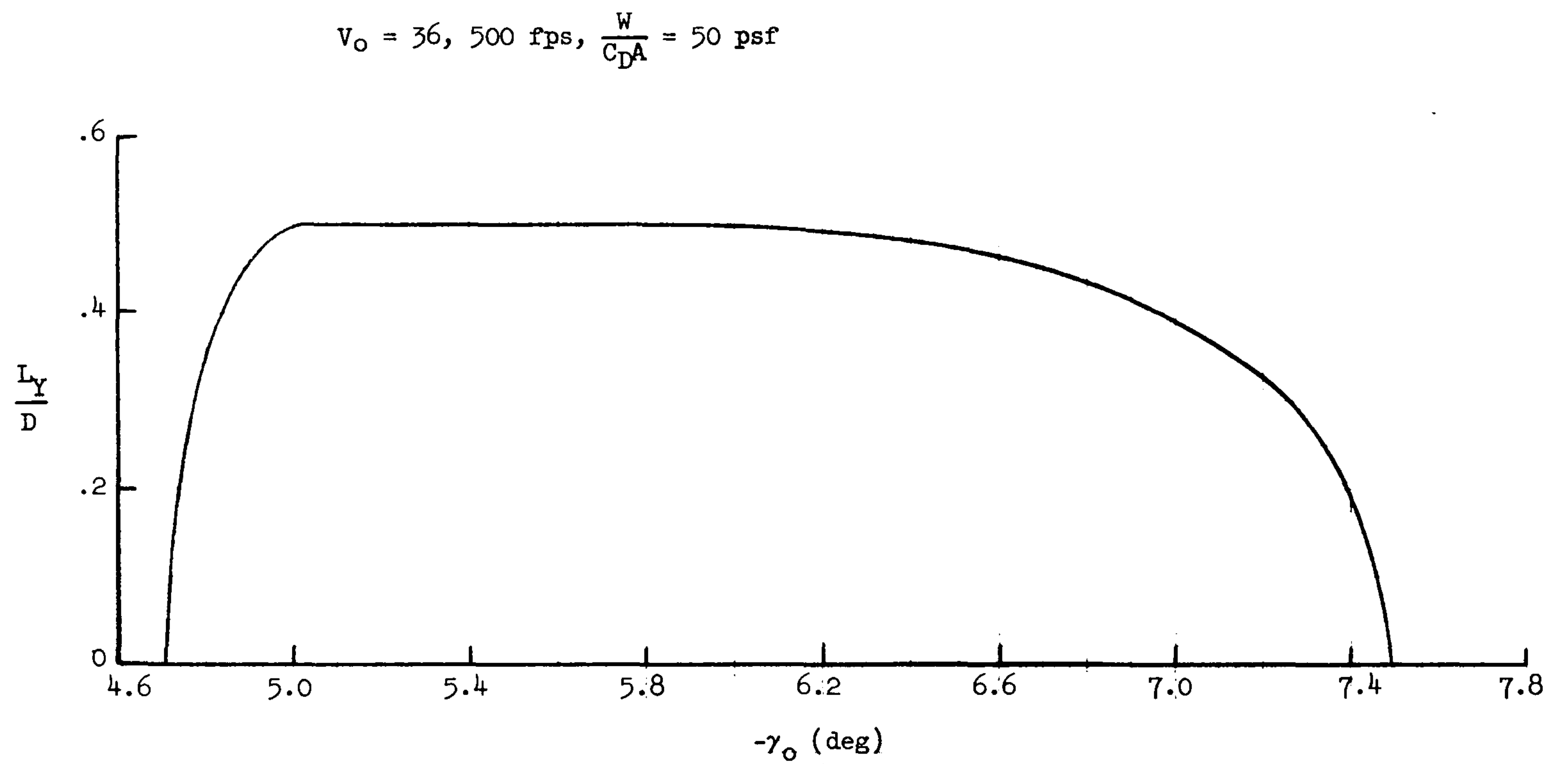

Figure 8.- Available side force during pull-up.

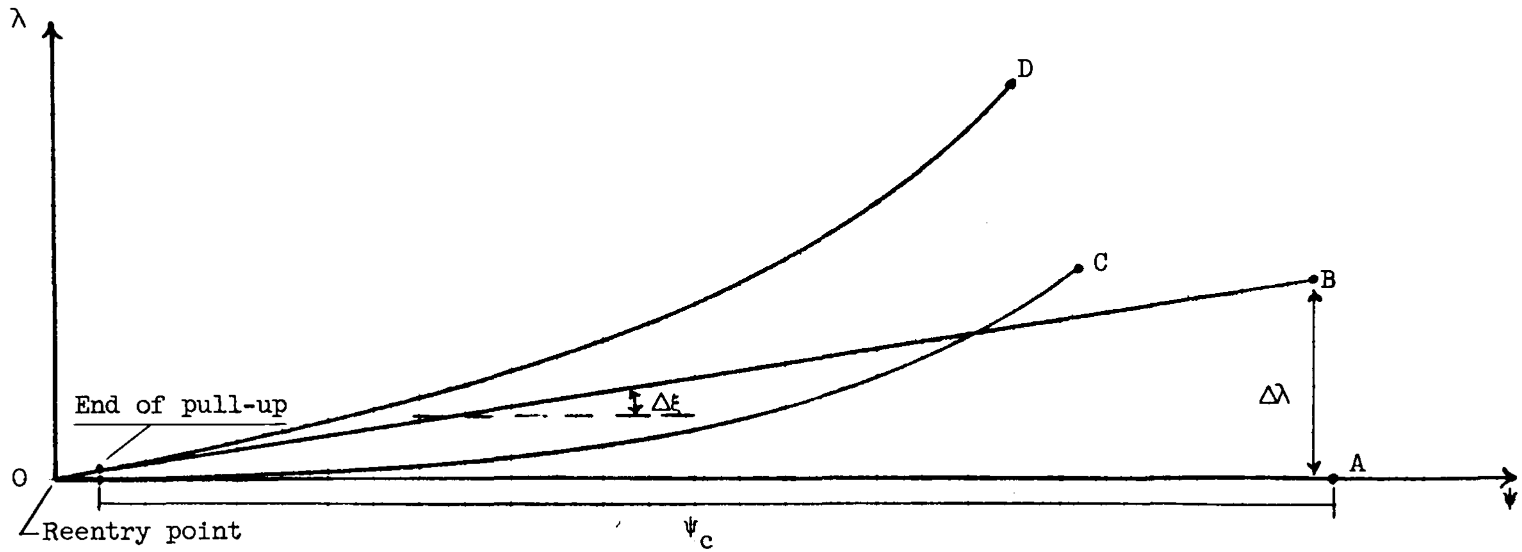

Figure 9.- Use of bank during pull-up to increase lateral range.

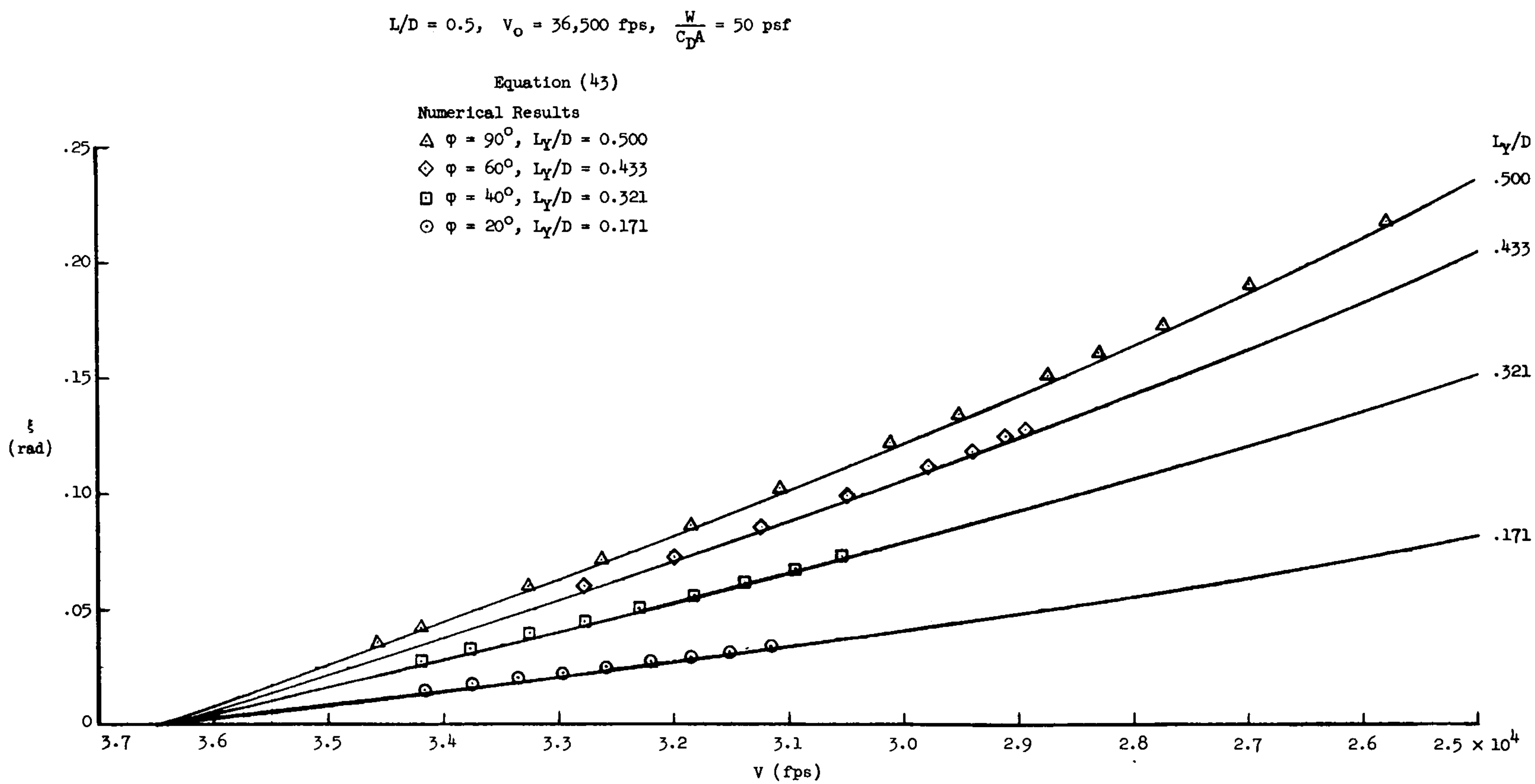

Figure 10.- Heading angle change during pull-up.

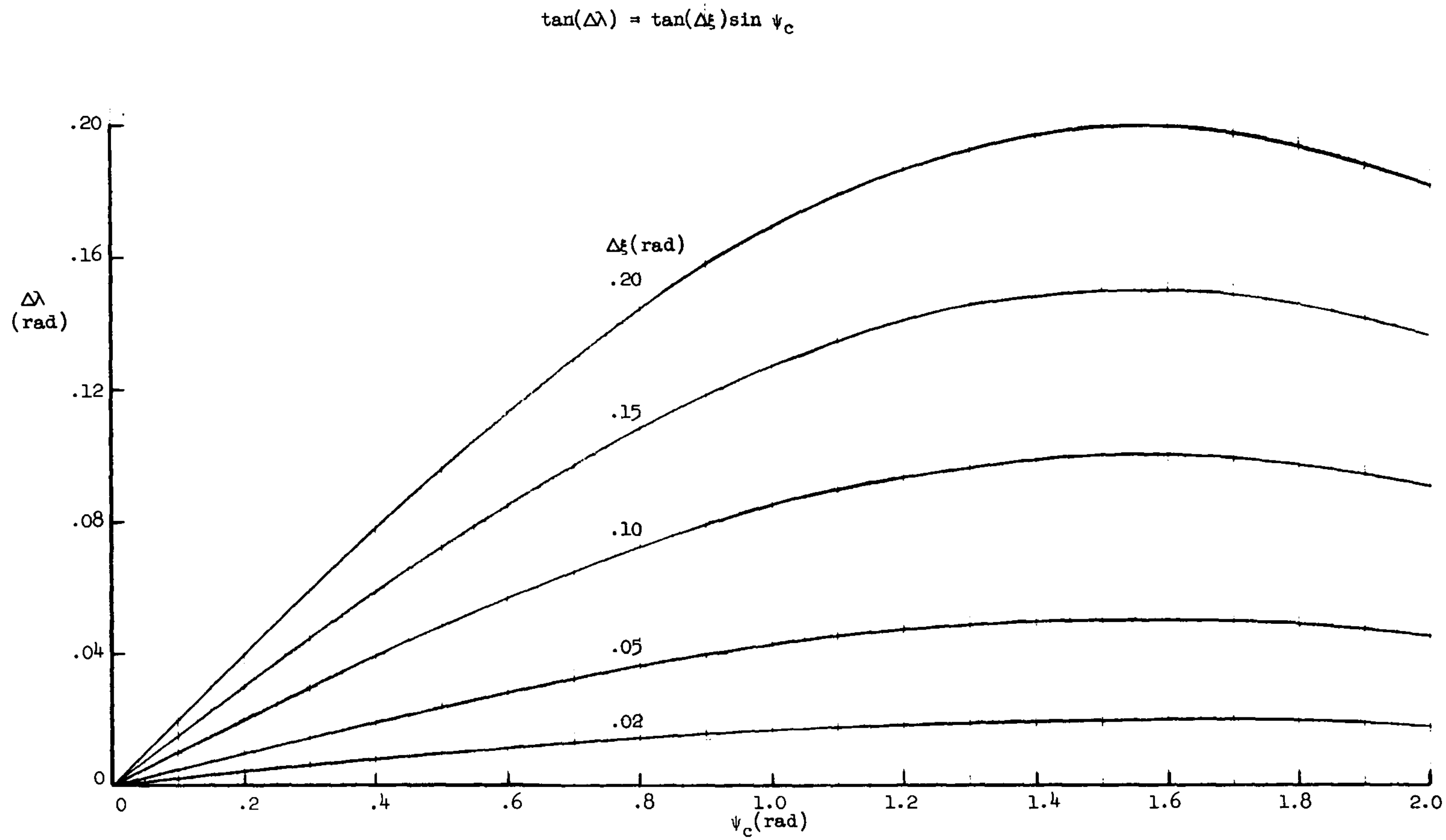

Figure 11.- Lateral range increment due to banked pull-up.

RANGE CONTROL DURING INITIAL PHASES OF

SUPERCIRCULAR REENTRIES

by

Donald Louis Baradell

ABSTRACT

For direct reentry from a lunar or deep space mission, considerable variation in reentry plane, reentry point, and reentry angle must be anticipated. The returning vehicle must therefore, possess the ability to control its range after reentry in order to touch down in the desired recovery area.

Recent studies have indicated that considerable ranging capability is available with even low lift-drag ratio vehicles operating wholly within the atmosphere if aerodynamic maneuvering is initiated while the vehicle still possesses greater than satellite velocity. In these studies, maneuvering was initiated shortly after the initial pull-up. Range control is also available during the initial pull-up, but such control results in little gain in longitudinal ranging capability in most cases.

It is the purpose of the present thesis to investigate the feasibility of increasing lateral ranging capability by banking during the initial pull-up. Low lift-drag ratio vehicles reentering the atmosphere in a banked attitude are considered and the effects of such reentries on allowable corridor width, and lateral range capability are studied.

Equations are developed for the motion of a vehicle reentering the atmosphere of a spherical, nonrotating earth, and some permissible approximations applicable for the present problems are discussed. Numerical results obtained for the developed system of equations through use of an IBM 7090 high-speed computer are used throughout the investigation to furnish accurate evaluations of the effects being studied and to check the validity of some of the approximations used.

Particular emphasis is placed on reentry at escape velocity, but the effects determined apply in character to reentry at other super-circular velocities.